Int J Pharm Bio Sci 2014 Jan; 5(1): (P) 84 - 94

Research Article **Medicinal Chemistry**

International Journal of Pharma and Bio Sciences

ISSN 0975-6299

PHARMACOPHORE DEVELOPMENT, ATOM BASED 3-D QSAR AND MOLECULAR DOCKING OF AURORA A KINASE INHIBITORS

CHANDRAKANT G. BONDE*

Department of Pharmaceutical Chemistry School of Pharmacy & Technology Management,SVKM's, NMIMS, Shirpur,Dist. Dhule,Maharashtra 425405 INDIA

ABSTRACT

Pharmacophore development, 3D-QSAR and docking studies were performed on twenty eight pyrrolotriazine derivatives as Aurora A kinase inhibitors. Five point pharmacophores with one hydrogen bond acceptor (A2), two hydrogen bond donor (D8, D11), one positive ionic (P15) and one aromatic ring (R17) as pharmacophoric features were developed. Amongst them the Pharmacophore hypothesis ADDPR.55 yielded best survival score 4.687 and was considered to be the best pharmacophore hypothesis. Correlation coefficient of experimental versus predicted K_d of training and test sets is 0.933 & 0.942 respectively. The atom based 3D QSAR was developed with good fitness (r^2= 0.9197), efficiency (q^2= 0.6372), fisher (F=51.5) and Pearson-R (0.9444). Further the hypothesis was validated by studying the interaction between the ligands and the receptor. The features identified in the pharmacophore showed good interaction between the pharmacophoric site points and the receptor residues. The geometry and features of pharmacophore were expected to be useful for the design of Aurora A kinase inhibitor.

KEYWORDS: **Pharmacophore, 3-D QSAR, PHASE, Aurora A kinase**

CHANDRAKANT G. BONDE
Department of Pharmaceutical Chemistry, School of Pharmacy & Technology Management,SVKM's, NMIMS,Shirpur,Dist. Dhule,Maharashtra 425405 INDIA

***Corresponding author**

1.0 INTRODUCTION

Aurora kinases belong to family of serine/threonine kinases that are essential for coordinated mitotic progression [1]. Aurora A & B is appropriate drug targets for cancer therapeutic armamentarium and these inhibitors called as antineoplastics or as targeted agents capable of modulating the cell toxicity. Aurora A, B and C are members of the Aurora kinase family have been identified [2]. The biological roles of Aurora A and B are identified and the role of Aurora C is still unclear. Experimental data suggest that inappropriately high or low levels of aurora kinase activity are linked to genetic instability [3]. Aurora A and B are essentially nonoverlapping due to their sequence homology and common association with cycling cells. Aurora A has well-established but perhaps not yet fully understood roles in centrosome maturation, duplication, mitotic entry and bipolar spindle assembly. Aurora A kinase spreads to mitotic spindle poles and midzone microtubules during metaphase[4]. After the breakdown of the nuclear envelope, inactive cytoplasmic aurora A is transported to the proximal ends of the microtubules and activated by the spindle protein TPX2 [5]. Aurora A is also involved in the process of G2-M transition with suppression of expression leading to G2-M arrest and apoptosis. The chromosomal passenger complex shows the accurate segregation of the chromatids at mitosis, histone modification and cytokinesis [6, 7]. Inhibition of Aurora A causes defects in centrosome separation with the formation of characteristic monopolar spindles [8]. Experimentally wide range of tumor types compared with essentially nonproliferating matched normal tissue and aurora A shows is strongly expressed at high frequency for anticancer activity [9].Pharmacophore modeling has been one of the important and successful approaches for new drug discovery. A pharmacophore is concept in rational drug design that underlies the importance of specific molecular features that favor the interaction with a particular enzyme or receptor active sight[10]. Pharmacophore methods use to identify pharmacophoric features like atoms or functional groups that can potentially interact with atoms in the binding site and then aligning the active conformations of the molecules such that their corresponding pharmacophoric features are overlaid [11, 12].PHASE, Pharmacophore Alignment and Scoring Engine (PHASE) is a comprehensive, self contained system for pharmacophore perception, 3D-QSAR model development and 3D database screening. PHASE uses a range of scoring techniques and fine-grained conformational sampling to generate and identify common pharmacophore hypothesis, which convey characteristics of 3-D chemical structures that are essential for binding [13]. Generated hypothesis with the aligned conformations may be combined with known activity data to create a 3D-QSAR model that identifies overall aspects of molecular structure that govern activity [14]. The objective of the present study is to develop ligand-based pharmacophore hypothesis and to derive atom-based 3D-QSAR model to update the designed process for Aurora A kinase inhibitors.

2.0 MATERIALS AND METHODS

2.1 Structure preparation

A set of 28 pyrrolotriazines analogs synthesized and evaluated by Abraham S. *et.al* as highly potent pan-Aurora A kinase inhibitors with available K_d data was taken from literature for the development of ligand-based pharmacophore and atom-based 3D-QSAR model [15] (Table 1). The biological activity data was reported as K_d (nM). The 2D structures were drawn using ChemAxon Marvin Sketch software and biological activity data was taken as negative logarithmic format.

Table 1
Chemical structures of compounds 1–28 with binding energy data (K_d)

Sr. No.	Compound ID	Structure	K_d	pK_d	QSAR set
1	12a	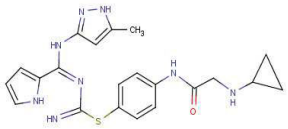	32	-1.505	Training
2	12b	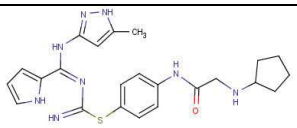	143	-2.155	Training
3	12c	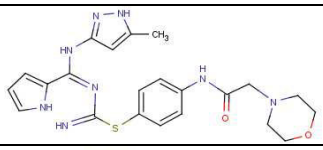	85	-1.929	Training
4	12d	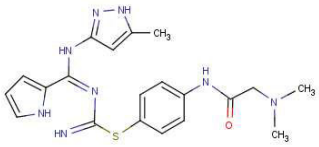	31	-1.491	Test
5	12e	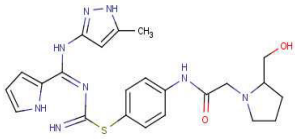	14	-1.146	Training
6	9a	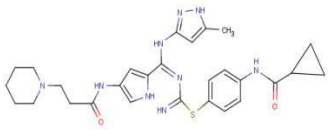	38	-1.579	Training
7	9c	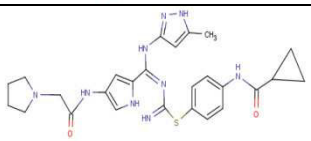	23	-1.361	Training
8	9d	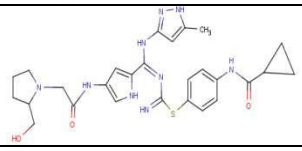	10	-1	Training
9	9e	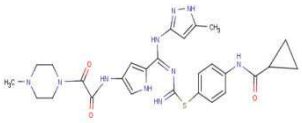	7	-0.845	Test
10	16a	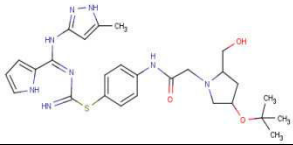	9	-0.954	Training
11	16c	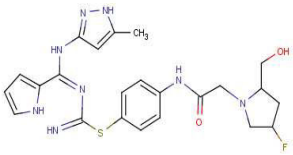	15	-1.176	Training

12	16e	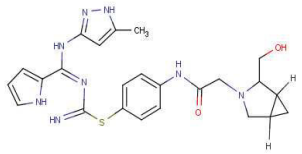	17	-1.230	Test
13	16f	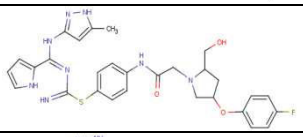	53	-1.724	Training
14	16h	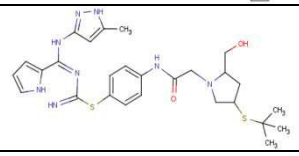	111	-2.045	Training
15	16i	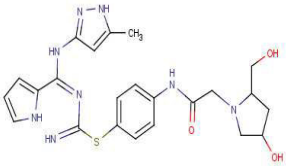	58	-.1.763	Training
16	17a	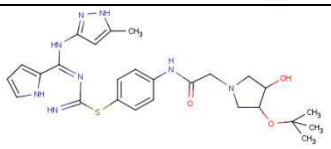	12	-1.079	Test
17	17c	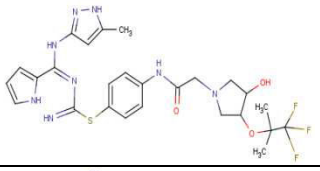	6	-0.778	Training
18	17d	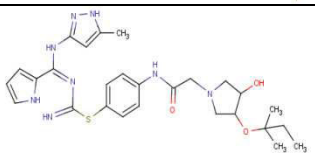	8	-0.903	Training
19	17e	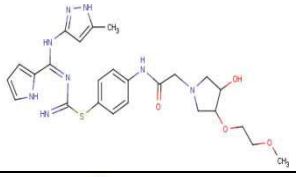	5	-0.698	Test
20	17f	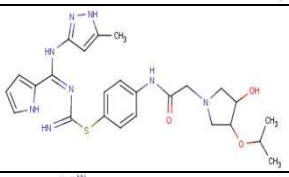	8	-0.903	Training
21	17g	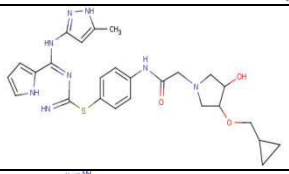	7	-0.845	Training
22	17h	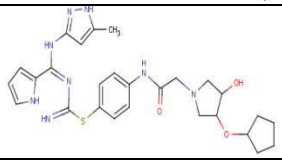	11	-1.041	Training

23	17i	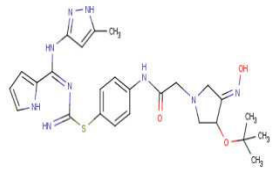	9	-0.954	Training
24	17j	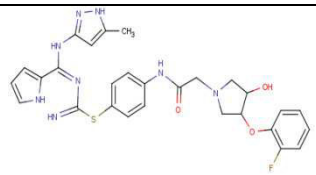	10	-1	Training
25	17k	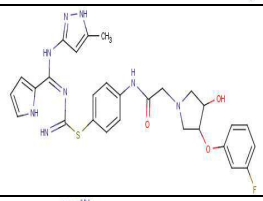	17	-1.230	Training
26	17l	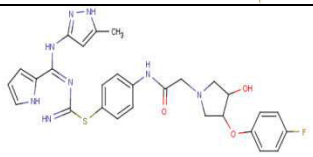	15	-1.176	Training
27	17m	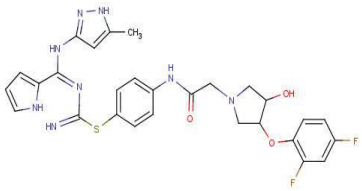	13	-1.113	Training
28	17n	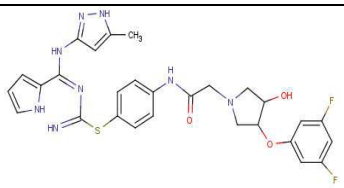	16	-1.414	Training

2.2 Ligand preparation

The total experiment was carried out by using Shordinger 8.0 molecular modeling software running over Windows OS. Geometry optimized by Macromodel program v 8.0 (Schrodinger, LLC) using the Optimized Potentials for Liquid Simulations (OPLS-2005) force field [16]. Partial atomic charges were computed using the OPLS-2005 force field. All the conformations were prepared using confgen alogorithm and taken as a one group for pharmacophore development.

2.3 Pharmacophore Development

Ligands were imported in PHASE module for the development of Pharmacophore model. The pharmacophore model was developed using a set of pharmacophore features to generate sites for all the compounds. Active compounds are normally considered during common pharmacophore hypothesis generation and thus pharmaset was defined by setting threshold. Five point common pharmacophore hypotheses were identified from all conformation of the active ligands having identical set of features with very similar spatial arrangement. Each structure is represented by a set of points in 3D space, which coincides with various chemical features that may make easy non-covalent binding among the ligand and its binding pocket. A large number of conformers were generated by Configen program and used to find and scoring of various sites like Hydrogen bond Acceptor (A), Aromaticity (R), Hydrogen bond donor (D)and Hydrophobicity (H) etc. The best hypothesis was selected on the basis of the fitness score and other relevant results like survival score, posthoc score and survival

minus inactive score which ensure their feasibility.

2.4 3-D QSAR

On the basis of the pharmacophore hypothesis based alignment a atom based 3D QSAR model was generated. By keeping 80% molecules of total set in training and rest in test set. This representation gives rise to binary-valued occupation patterns that can be used as independent variables to create partial least-squares (PLS) 3D-QSAR models.. The 3DQSAR was evaluated by cross validated correlation coefficient (r2 CV), standard error of estimation (SD), Fisher test (F), correlation coefficient (r2) and Person (R).

2.5 Protein structure preparation

The X-ray crystal structure of Aurora A kinase in complex with compound 26 (PDB ID: 3P9J) obtained from the RCSB Protein Data Bank (PDB) was used in order to model the protein structure in this study. Water molecules of crystallization were removed from the complex, and the protein was optimized for docking using the protein preparation and refinement utility provided by Schrodinger LLC.

Table 2
Parameters of five pharmacophore hypothesis

ID	Survival	Survival -inactive	Post-hoc
ADDPR.55	**4.687**	**2.378**	**3.329**
ADDRR.82	4.683	2.484	3.325
DDRRR.172	4.664	2.499	3.306
ADDRR.83	4.662	2.428	3.304
DDPRR.118	4.658	2.385	3.3

Table 3
The experimental K_d (Exp.), predicted K_d (Pred.) and their residuals (Res.) of the active and inactive set molecules

ID	Exp.	Pred.	Res.	Set	ID	Exp.	Pred.	Res.	Set
12a	32	36.3	-4.3	I	16i	58	28.1	29.9	I
12b	143	147	-4	I	17a	12	18.1	-6.1	*
12c	85	58	27	I	17c	6	4.4	1.6	A
12d	31	38	-7	*	17d	8	8.1	-0.1	A
12e	14	23	-9	*	17e	5	9.3	-4.3	A
9a	38	39.8	-1.8	I	17f	8	8.7	-0.7	A
9c	23	22.3	0.7	*	17g	7	8.3	-1.3	A
9d	10	7.5	2.5	A	17h	11	11.2	-0.2	*
9e	7	10.2	-3.2	A	17i	9	9.77	-0.77	A
16a	9	7.9	1.1	A	17j	10	12.3	-2.3	A
16c	15	24.5	-10.5	*	17k	17	15.4	1.6	*
16e	17	15.4	1.6	*	17l	15	17.3	-2.3	*
16f	53	44.6	8.4	I	17m	13	14.7	-1.7	*
16h	111	109.6	1.4	I	17n	16	26.3	-10.3	*

A- Active, I- Inactive, * -Moderately active

Table 4
Statistic parameters for 3D QSAR

Run	SD	R square	F	P	RMSE	Q Square	Pearson R
1	0.1189	0.9318	61.5	2.991e-010	0.235	0.3838	0.8511
2	0.1094	0.9343	64	2.138e-010	0.3086	0.4549	0.7014
3	0.1265	0.9197	51.5	1.292e-009	0.1686	0.6372	0.9444

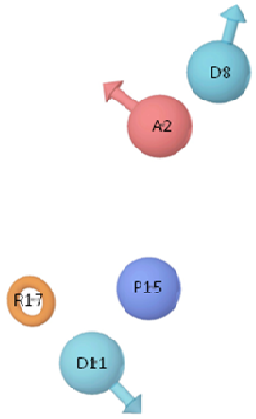

Figure 1
Common pharmacophore hypothesis 26 based alignment of the whole set compounds. Pharmacophore features are red vector for hydrogen-bond acceptors (A), light blue vectors for hydrogen-bond donors (D), blue for positive ionic (P),orange rings for aromatic groups (R).

Table 5
Distances between different sites of model ADDPR.55

Site1	Site2	Distance
A2	D8	6.337
A2	D11	2.094
A2	P15	4.096
A2	R17	5.726
D8	D11	8.21
D8	P15	2.696
D8	R17	2.212
D11	P15	5.756
D11	R17	7.795
P15	R17	3.431

Table 6
Angles between different sites of model ADDPR.55

Site1	Site2	Site3	Angle	Site1	Site2	Site3	Angle
D8	A2	D11	149.5	D8	D11	P15	9.3
D8	A2	P15	16.9	D8	D11	R17	15.6
D8	A2	R17	20.3	P15	D11	R17	23.8
D11	A2	P15	134.2	A2	P15	D8	136.8
D11	A2	R17	169.5	A2	P15	D11	15.1
P15	A2	R17	36.3	A2	P15	R17	98.7
A2	D8	D11	7.4	D8	P15	D11	150.5
A2	D8	P15	26.2	D8	P15	R17	40.1
A2	D8	R17	64.1	D11	P15	R17	113.7
D11	D8	P15	20.2	A2	R17	D8	95.6
D11	D8	R17	71.5	A2	R17	D11	2.8
P15	D8	R17	88.1	A2	R17	P15	45
A2	D11	D8	23.1	D8	R17	D11	92.9
A2	D11	P15	30.7	D8	R17	P15	51.8
A2	D11	R17	7.7	D11	R17	P15	42.6

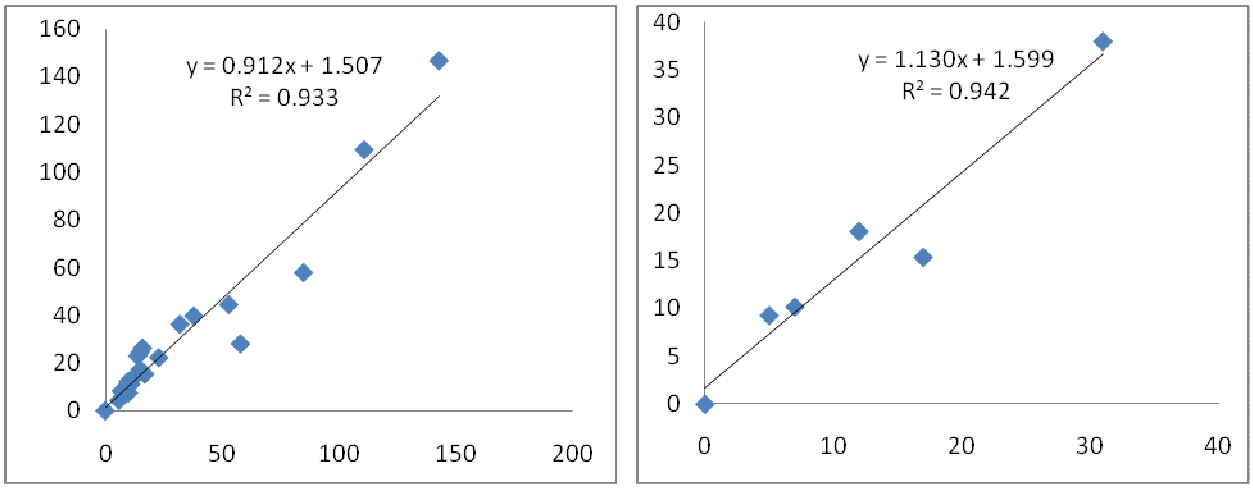

(A) (B)

Figure 2

***Correlation graph of actual versus predicted K_d of the training set (A) and the test set* (B).**

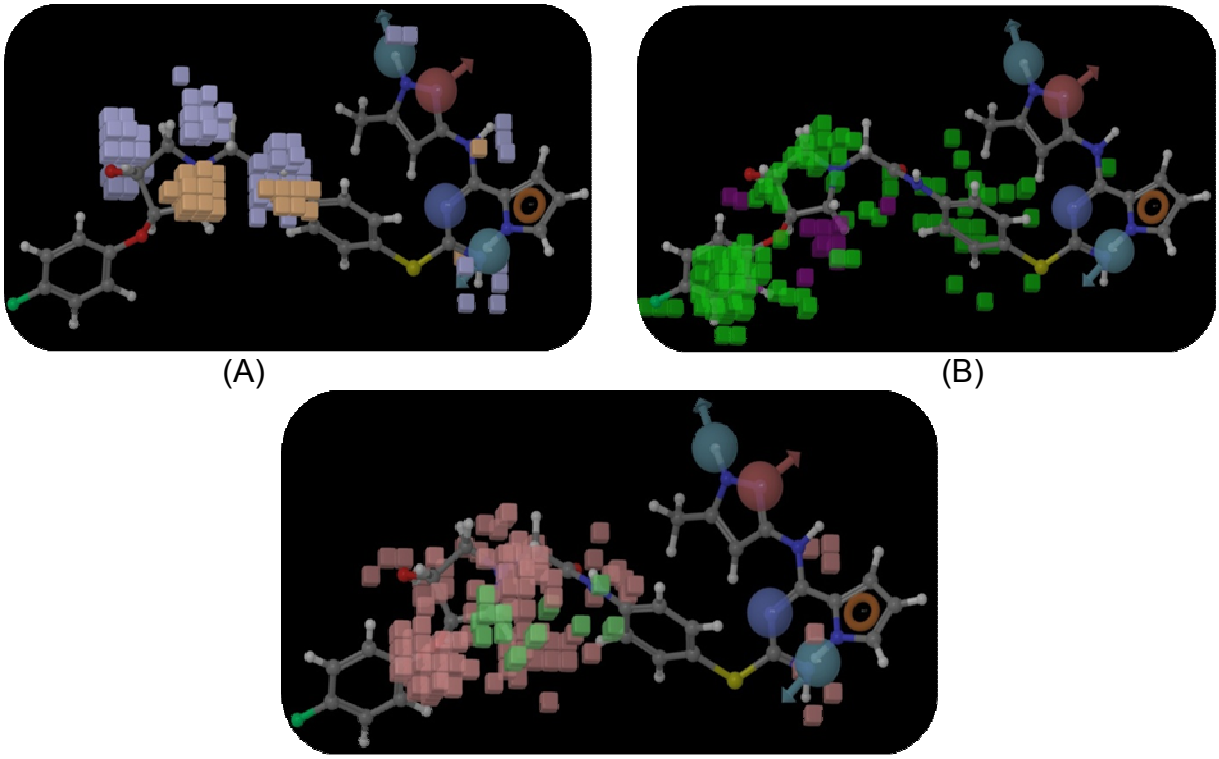

(A) (B)

(C)

Figure 3

Visual representation of atom-based 3D-QSAR model in context of the most active compound 26. (A) Hydrogen bond donor, light blue cube indicates positive coefficient (increase in activity), orange cube indicates negative coefficient (decrease in activity); (B) Hydrophobic, green cube indicates positive coefficient, purple cube indicates negative coefficient; (C) Electron-withdrawing, pink cube indicates positive coefficient, light green cube indicates negative coefficient.

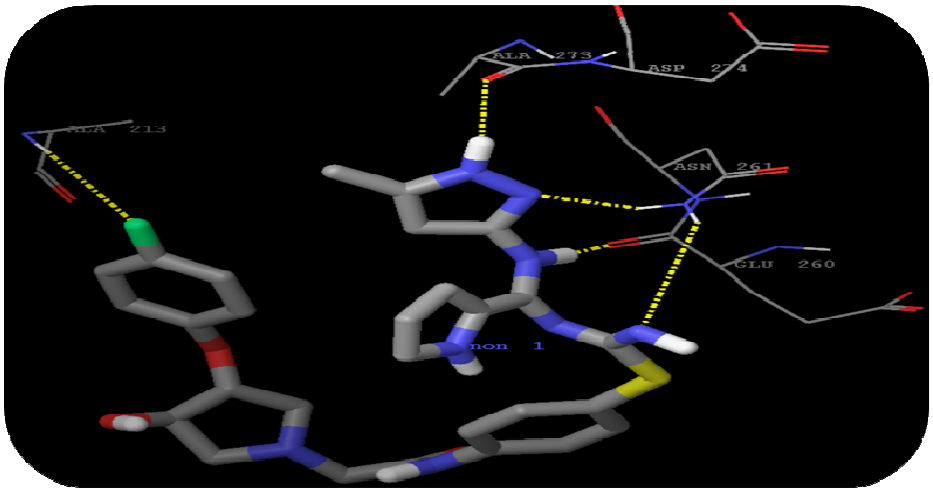

Figure 4
Docked binding modes of compound 26 in the binding site of Aurora A kinase. Key residues and hydrogen bonds are distinctly labeled.

3.0 *Result and Discussion*

The best model was found to be associated with five-point hypothesis, which consists of one hydrogen bond acceptors (A), two hydrogen bond donor (D), one positive ionic (P) and one aromatic ring (R) denoted as A2, D8, D11, P15 and R17 (Fig 1). From all hypotheses, ADDPR.55 hypothesis was selected on the basis of highest survival score (4.687) which ensure their feasibility and it can nicely describe the pharmacophoric features of all compounds (Table 2). This pharmacophoric features was used to align all the molecules for 3D QSAR analysis. For the 3D-QSAR models generation activity threshold was set to distinguish the active(above -1.000), inactive (below -1.500) and moderately active ligands. (Table 3). The distances and angles between different sites of ADDPR.55 are given in (Table 5 and 6) respectively.The best pharmacophore hypothesis was used to find out atom based 3D QSAR model by keeping 80% molecules in training set and rest in test set (Table 1). The statistical result of the atom based 3D QSAR model was quite good and its external validation further proved it's statistically significance. The result at PLS factor 4 was SD = 0.1265, R^2 = 0.9197, F = 51.5, Q^2 = 0.6372 and Pearson R = 0.9444 (Table 4). The predicted K_d and experimental K_d are tabulated in Table 3. Correlation coefficient (r2) of Experimental versus predicted K_d of training and test sets are 0.933 and 0.942 respectively (Fig 2A&B)

3.1 3-D QSAR Analysis

Additional insight into the Aurora A kinase inhibitor activity can be gained by visualizing the 3-D QSAR model in the context of one or more ligands in the series with varying activity. This information can then be used to design new or more active analogues. 3-D QSAR models based on the molecules of training and test set using various features, i.e., hydrogen bond acceptor (A), hydrogen bond donor (D), hydrophobic regions (H) and electron withdrawing group (E) has been studied. Thus the developed model is a statistically relevant model which can add an edge to anticancer drug research for the development of potent anticancer agents. A pictorial representation of the cubes generated in the present 3D-QSAR of active ligand 26.

3.1.1. Hydrogen bond donor field predictions

The 3-D QSAR model based on molecule 26 of the training set using hydrogen bond donor feature is shown in Fig 3 (A). Light blue region near and around the hydrogen of triazine & pyrazole indicates that the substitutions at these positions by groups having more hydrogen bond donor property favors the aurora A kinase inhibitor activity. Orange region around the N in

pyrrole and benzene ring attached to sulphur indicates that substitutions at these positions by groups having hydrogen bond donor property do not favors aurora A kinase inhibitor activity. The light blue cubes around D11 and D8 of the most active compound 26 suggest that substitution at H donor nitrogen is favorable for biological activity. Further substitution at N of pyrazole in same vector significantly increased the activity. At main ring triazine, light blue cubes are observed and it shows substitution on triazine ring potentiates the biological activity.

3.1.3 Hydrophobicity field prediction

The 3-D QSAR model based on molecule 26 of the pharm set using hydrophobic feature is shown in Fig 3 (B). Green region around benzene ring substituted at acetamide, sulphur attached benzene ring and hydroxyl group at pyrrole ring attached to acetamide indicates that the substitutions at these positions by groups having more hydrophobicity, favors aurora A kinase inhibitory activity. Purple region around pyrrole ring indicates that groups having more hydrophobic property do not favor aurora A kinase inhibitor activity. Hydrophobic interaction is not observed in pharmacophoric site but halogen substitution at site other than phamacophoric site increase in biological activity.

3.1.3 Electron withdrawing field prediction

The 3-D QSAR model based on molecule 26 of the pharm set using electron withdrawing feature is shown in Fig 3 (C). Red cubes near to triazine ring indicate that substitution at this site increase in binding activity of arurora A kinase inhibitor. Substitution at acetamide with electron withdrawing group may increase binding affinity with receptor.

3.2 Molecular Docking

To substantiate the phamacophoric model , the ligands were docked with the protein. Molecular docking performed with PDB 3P9J and ligands. The pose of the most active ligand 26 is shown in Fig. 4. The pyrazole ring showed the hydrogen bonding with ALA273, ASN261 and nitrogen attached to pyrazole ring binds with GLU260 through hydrogen bond. Pyrazole –N– and –NH ring atoms form hydrogen bonds with ASN261 (–N_ HN, Distance = 2.239 A°) and ALA273 (– NH_ O, Distance = 2.152A°) backbone respectively. Nitrogen of triazin shows hydrogen binding with ASN261 and distance between –N–_ HN is 2.823. The 5-amino function of the pyrrolo 1,2,4 triazin ring forms a hydrogen bond with the backbone GLU260 (–NH_ O). The fluorine at the 4 of benzene ring position forms a hydrogen bond with the ALA213 side chain (F_ H_2N) located in the upper lobe of the highly solvent-exposed phosphate binding site of Aurora A kinase. All pharmacophoric sites which show H bond donor features in 3-D QSAR are binding with same features in molecular docking.

3.0 CONCLUSION

This study shows the generation of a pharmacophore model ADDPR.55 for pyrrolotriazine acting as Aurora A kinase inhibitor. Pharmacophore modelling correlates activities with the spatial arrangement of various chemical features. The first hypothesis ADDPR.55 is the best hypothesis in this study, characterized by the best regression coefficient (0.9197), degree of freedom (51.5) and highest survival score (4.687). Hypothesis ADDPR.55 represents the best pharmacophore model for determining Aurora A kinase inhibitor activity. ADDPR.55 consists of one hydrogen bond acceptor, two hydrogen bond donor, one positive ionic region and one aromatic ring features. ADDPR.55 model had strong correlation between experimental and estimated activity of the training (R2 = 0.933) and test (R2 = 0.942) set molecules. Thus, ADDPR.55 pharmacophore model was able to accurately predict Aurora A kinase inhibitor activity and the validation results also provide additional confidence in the proposed pharmacophore model. Pyrazole –N– and –NH and nitrogen of trazine show H bond binding with ASN261, ALA273 and ASN261 respectively. The distance observed between these binding was found to be 2.239, 2.152 and 2.823 A^0 respectively. The obtained results suggested that the proposed 3-

D QSAR model ADDPR.55 can be useful to rationally design new pyrrolotriazine molecules as Aurora A kinase inhibitor and also to identify new promising molecules as Aurora A kinase inhibitor in large 3-D database of molecules.

5.0 REFERENCES

1. M. Li, A. Jung, U. Ganswindt, P. Marini, A. Friedl, P.T. Daniel, K. Lauber, V. Jendrossek, C. Belka, Biochemistry Pharmacology, 2010, 79, 122 - 129.
2. J.R. Medina, S.W., Grant, J.M., W.H. Miller, C.A. Donatelli, M.A. Hardwicke, C.A. Oleykowski, Q. Liao, R. Plant, H. Xiang, Bioorganic Medicinal Chemistry Letters, 2010, 20, 2552 - 2555.
3. R. Giet , C. Petretti, C. Prigent, Aurora kinases aneuploidy and cancer A coincidence or a real link, Trends Cell Biology, 2005, 241 - 50.
4. J. Fu, M. Bian, Q. Jiang, C. Zhang, Roles of aurora kinases in mitosis and tumorigenesis, Molecule Cancer Research, 2007, 1 - 10.
5. P.D. Andrews, Aurora kinases: shining lights on the therapeutic horizon, Oncogene, 2005, 5005 - 15.
6. M. Cazales, E. Schmitt, E. Montembault, C. Dozier, C. Prigent, B., CDC25B phosphorylation by aurora-A occurs at the G2/M transition and is inhibited by DNA damage, Cell Cycle, 2005, 1233 - 8.
7. J. Du, D.J. Hannon, Suppression of p160ROCK bypasses cell cycle arrest after aurora-A/STK15 depletion, Proceedings of National Academy Science, USA, 2004, 8975 - 80.
8. N.D. Adams, J.L. Adams, J.L. Burgess, A.M. Chaudhari, R.A. Copeland, C.A. Donatelli, D.H., Journal of Medicinal Chemistry, 2010, 53, 3973 - 4001.
9. S. Wang, C.A. Midgley, F. Scaerou, J.B. Grabarek, G. Griffiths, W. Jackson, G., D.M. Glover, P.M. Fischer, Journal of Medicinal Chemistry, 2010, 53, 4367 - 4378..
10. D.P. Marriott, I.G. Dougall, P. Meghani, Y.J. Liu, D.R. Flower, Journal of Medicinal Chemistry, 1999, 42, 3210 - 3216.
11. T.T Talele, S.S. Kulkarni, V.M. Kulkarni, Journal of Chemistry Computer Science, 1999, 39, 958–966.
12. R.G. Karki, V.M. Kulkarni, European Journal of Medicinal Chemistry, 2001, 36, 147–163.
13. Phase, version 3.1, Schrödinger, LLC, New York, USA, 2009.
14. Maestro, version 9.0, Schrödinger, LLC, New York, USA, 2009.
15. S. Abraham, H. Hua, M.D. Cramer, D.K. Treiber, Novel series of pyrrolotriazine analogs as highly potent pan-Aurora A kinase inhibitors, Bioorganic & Medicinal Chemistry Letters, 2011, 21, 5296 – 5300.
16. S.L. Dixon, A.M. Smondyrev, E.H. Knoll, S.N. Rao, D.E. Shaw, Journal of Computer-Aided Molecular Design, 2006.